Composites Part C: Open Access 8 (2022) 100257

Contents lists available at ScienceDirect

Composites Part C: Open Access

journal homepage: www.sciencedirect.com/journal/composites-part-c-open-access

Shear strength of recycled-aggregate concrete beams with glass-FRP stirrups

Adel Younis [a,*], HossamEldin El-Sherif [b], Usama Ebead [c]

[a] Postdoctoral Fellow, Department of Building Technology, Faculty of Technology, Linnaeus University, P. O. Box 35195, Växjö, Sweden
[b] Graduate Research Assistant, Department of Computational Data Science and Engineering, North Carolina A&T State University, 1601 E Market St, Greensboro, NC 27411, Greensboro, NC, United States
[c] Professor, Department of Civil and Architectural Engineering, College of Engineering, Qatar University, P. O. Box 2713, Doha, Qatar

ARTICLE INFO

Keywords:
Recycled concrete aggregate
GFRP reinforcement
Shear behavior
Reinforced concrete beams
Sustainable construction

ABSTRACT

The combined use of recycled concrete aggregate (RCA) and glass fiber reinforced polymer (GFRP) reinforcement in reinforced concrete (RC) structures is deemed plausible to achieve sustainable construction. This paper aims to examine the effect of such a combination (RCA + GFRP reinforcement) on the shear behavior of RC beams. Six medium-scale RC beams (150 × 260 × 2200 mm) critical in shear were tested under three-point loading until failure. The test variables were the aggregate type (natural/recycled) and the shear reinforcement (steel/GFRP/none). The failure modes, cracking patterns, load-carrying capacities, deformational and strain characteristics were analyzed and compared among the tested specimens. It was found that using 100% RCA in the concrete mix reduced the shear strength of RC beams (by 12% on average). Minor effects were observed on the shear strength of the beam specimens (~2%) with altering the transverse reinforcement (GFRP versus steel). Theoretical load-carrying capacities of the tested beams were obtained as per contemporary design guides and compared with the experimental results.

1. Introduction

Concrete is the most commonly used construction material worldwide [1], primarily composed of cement, freshwater, and natural aggregates (fine/coarse). Given the high volumes of concrete produced, the current practices to generate concrete from its raw ingredients involve significant environmental impacts [2,3]. The global construction industry uses considerable amounts of natural aggregates extracted from their natural resources to produce concrete (over 40 billion tons annually [4]). Besides, the construction and demolition activities account globally for over two billion tons of solid wastes every year that, unless recycled, may lead to severe environmental and economic impacts [4]. Consequently, there is a growing interest among researchers and practitioners in finding alternative sustainable solutions to produce concrete, e.g. recycled concrete aggregates (RCA) [5].

Corrosion of steel reinforcement in concrete structures remains a critical challenge that causes premature structural deterioration and reduces the service life of existing structures. The global cost of corrosion has been recently estimated at $2.5 trillion, around 35% of which is accounted for damages in services and infrastructure [6]. While several strengthening materials and techniques have been proposed to restore the structural capacity of vulnerable concrete (e.g. textile reinforced mortar [7], ferrocement [8], fiber-reinforced polymer [9]), such retrofitting measures may be time-consuming, labor-intensive, and often impractical to apply on existing structures. Therefore, the use of non-corrosive reinforcement at the construction stage, such as glass fiber reinforced polymer (GFRP), is deemed promising [10]. In the past few decades, GFRP has emerged as an alternative non-corrosive reinforcement for concrete given its relatively low cost (compared to stainless steel or carbon-FRPs) as well as acceptable mechanical and durability performances [11].

Previous studies revealed significant environmental benefits associated with the use of RCA acquired from construction and demolition waste to produce new concrete [12–14]. For example, Hossain et al. [13] conducted a life-cycle-assessment study to assess the environmental implications of incorporating RCA in concrete, and reported potential savings of 65% in greenhouse gas emissions as well as 58% in non-renewable energy consumption. The use of GFRP reinforcement in structural concrete in place of traditional steel has also shown an advantage from a sustainability perspective, attributable to the

* Corresponding author.
E-mail addresses: adel.younis@lnu.se (A. Younis), haelsherif@aggies.ncat.edu (H. El-Sherif), uebead@qu.edu.qa (U. Ebead).

https://doi.org/10.1016/j.jcomc.2022.100257

Available online 23 March 2022

increased service life and reduced maintenance demands [15–18]. For instance, Cadenazzi et al. [15] performed an LCA study to compare a GFRP-reinforced concrete bridge in Florida with a conventional steel-reinforced counterpart at the design stage. The cradle-to-grave environmental impacts associated with the use of GFRP reinforcement were 25%, 15%, 5%, and 50% lower than those of the conventional design in terms of global warming, photochemical oxidant creation, acidification, and eutrophication, respectively. Apart from the environmental perspective, combining RCA and GFRP may also result in significant cost benefits in the long term. Younis et al. [19] reported 40–50% life-cycle cost savings associated with the use of seawater-mixed recycled-aggregate GFRP-reinforced concrete in high-rise buildings as compared to conventional design (in which steel reinforcement, natural aggregates, and freshwater-mixed concrete are used).

Several researchers investigated the effects of using RCA on the shear performance of RC beams [20–29]. Arezoumandi et al. [30] studied the effect of using 100% RCA on the shear strength of RC beams considering different reinforcement ratios, and reported an average reduction of 10–15% in the shear strength associated with the use of RCA [30]. Choi et al. [23] tested 20 RC beams critical in shear with different span-to-depth ratios and RCA replacement levels (0–100% by weight): the test results revealed up to 30% reductions in the shear strength of RC beams and significant increases in deflections (especially at 100% replacement level) [23]. Likewise, Pradhan et al. [25] compared the shear performance of natural-aggregate and recycled-aggregate RC beams, considering the longitudinal reinforcement ratio and the presence/absence of stirrups as the test parameters. The particle packing method was implemented with a two-stage mixing approach to replace natural aggregates with RCA, which led to improved mechanical properties of recycled-aggregate concrete. It was observed that the shear strength of concrete beams without stirrups decreased by 14% compared to that of natural-aggregate concrete, but no significant difference was reported with the use of RCA in case of RC beams with stirrups [25]. The decline in the shear strength associated with the use of RCA is mostly attributed to the natural reduction in the concrete's compressive strength, which may be counterbalanced by adjustments in the mixture design (e.g. lowering water-to-cement ratio) [31]. The implementation of certain by-products in the concrete mix may also improve the performance of recycled-aggregate concrete beams. For instance, De Domenico et al. [32] investigated the structural behavior of full-scale beams made of concrete with electric arc furnace (EAF) slag as recycled aggregates and compared them with RC beams made with natural aggregates. Some beams were designed to fail in bending and some others to fail in shear. It was observed that the EAF slag reduced the crack widths and increased the overall ductility of the RC beams. As far as the adequacy of the current design guides is concerned, Rahal and Elsayed [33] confirmed that the shear calculations of ACI [34], CSA [35], and EC2 [36] codes are conservative for recycled-aggregate concrete beams.

A significant amount of research was devoted to the shear behavior of RC beams with FRP stirrups [37–46]. Bentz et al. [47] examined the shear strength of GFRP-RC beams and reported that, despite the brittle behavior of GFRP reinforcement, the shear performance of GFRP-reinforced beams was similar to that of their steel-reinforced counterparts [47]. Likewise, Ahmed et al. [39] compared the shear strength among RC beams that varied in transverse reinforcement material (carbon-FRP, glass-FRP, and conventional steel) and considered different stirrups spacing. The test results revealed approximately 5% difference in the shear strength between specimens with GFRP and steel stirrups having the same diameter and spacing, but with a more brittle failure associated with the former (i.e. GFRP rupture Vs. steel yield) [39]. Other researchers reported notable reductions in the shear strength, though, with the use of FRP stirrups in place of steel stirrups for fiber-reinforced concrete beams with longitudinal FRP bars [48,49]. As far as the accuracy of the design guides is concerned, the CSA S6–06 [50] and ACI 440.1R-06 [51] provisions generally provide conservative predictions for the shear strength [39,47]. Likewise, previous research contributions [52–54] reported that the Eurocode EC2 model [36] is over-conservative in the shear-strength prediction of RC beams. In this context, De Domenico [52] proposed an upgrade/improvement for the shear strength equation of the EC2 [36] by introducing two variable-inclination compression struts in the truss mechanism underlying the Eurocode formulation to mitigate such conservativeness. More recently, machine-learning-based models have been proposed to predict the shear strength of FRP-RC beams [55]. The above-mentioned studies, however, did not investigate the effect of using RCA on the shear behavior of GFRP-RC beams.

Table 1
Concrete mixtures.

Property	Mix A	Mix B
1. Concrete mixture design		
Coarse Aggregates	Conventional — 686 kg/m^3 (Gabbro 20 mm) + 457 kg/m^3 (Gabbro 10 mm)	Recycled — 990 kg/m^3 (5–20 mm RCA)
Fine Aggregates	795 kg/m^3 (washed sand)	830 kg/m^3 (washed sand)
Ordinary Portland cement	126 kg/m^3	133 kg/m^3
Slag	234 kg/m^3	247 kg/m^3
Water	167 kg/m^3	186 kg/m^3
Superplasticizer (Polycarboxylate, liquid)	4.54 kg/m^3	5.40 L/m^3
2. Fresh and hardened properties		
Initial slump [72]	180 mm	180 mm
Density [73]	2454 kg/m^3	2373 kg/m^3
7-day compressive strength [74]	38.9 ± 0.2*MPa*	35.2 ± 2.5*MPa*
28-day compressive strength [74]	47.7 ± 0.6*MPa*	46.0 ± 1.8*MPa*
28-day flexural strength [75]	5.2 ± 0.3*MPa*	3.3 ± 0.2*MPa*

In view of the aforementioned literature survey, this paper is aimed at investigating the combined effects of using RCA and GFRP reinforcement on the shear performance of RC beams. As both steel and GFRP reinforcements are used in conventional concrete and their effects are well known, this effort is an attempt to verify whether any differences appear in the presence of RCA. For this, six RC beams critical in shear were tested under 3-point loading until failure. The test variables included the aggregate type (natural/recycled) and the transverse reinforcement material (none/steel/GFRP). Here, we maintained a comparable compressive strength between natural-aggregate and recycled-aggregate concretes by adjusting the mix design. This would neutralize the effects from the expected reduced compressive strength of recycled-aggregate concrete, and would keep the sole focus on the impact of using RCA per se. In addition, the shear-strength predictions were obtained in accordance with selected commonly used design guides, and compared with the experimental results.

2. Materials and methods

2.1. Concrete mixtures

Ready-mix concrete with a 40-MPa 28-day design compressive strength was considered. Two concrete mixtures were considered as shown in Table 1, namely, Mix A (reference) and Mix B. The former was mixed with natural coarse aggregates, while the latter was produced using coarse RCA at 100% replacement level. The chemical and mechanical characterization of the aggregates used can be found in Ref. [56], in which work the same aggregate resources were adopted. Blast furnace slag was incorporated in both mixtures, at a 65% replacement level of ordinary Portland cement, since it is proved to

Table 2
Test matrix for the RC beams.

Beam Code	Concrete Mix	C.S.S Stirrups
N-A	A	No stirrups
N-B	B	No stirrups
S-A	A	Steel stirrups
S-B	B	Steel stirrups
G-A	A	GFRP stirrups
G-B	B	GFRP stirrups

enhance the durability of recycled-aggregate concrete [57]. The chemical characterization of the cementitious materials (i.e. slag and Portland cement) can be found in Ref. [58], in which work the same cementitious materials were used.

The mix design proportions for each mixture as per BS EN 206 [59] are shown in Table 1. To determine the quantity of RCA replacing natural aggregates, the direct volume replacement method was used. A higher water amount was considered in Mix B to account for the increased water absorption of the RCA compared to natural aggregates. Both mixtures were designed to achieve similar initial slump and compressive strength: this was accomplished by reducing the w/c ratio (via ~6% increase in cement concentration) and increasing the superplasticizer dosage in Mix B (by ~20%). Table 1 lists the fundamental fresh and hardened properties for both concrete mixtures. The density of Mix B concrete was slightly lower than that of Mix A (by ~4%), consistent with previous studies on RCA concrete [60]. A 180-mm minimum initial slump was measured for both concrete mixtures. The 28-day compressive strength for Mix A and Mix B concretes was similar (47.7 MPa and 46 MPa, respectively). The flexural tensile strength of Mix A concrete, however, was higher than that of Mix B (by ~58%).

2.2. RC beam specimens

Table 2 presents the test matrix of the current study. Six RC beams were prepared and tested under 3-point loading until failure to evaluate their shear performance. The test variables considered were the mix design (Mix A or Mix B) and the shear reinforcement (none, steel, or GFRP) provided along the critical shear span (CSS). Each specimen was labeled as X-Y, where 'X' indicates the CSS stirrups (N: no stirrups, S: steel, or G: GFRP), and 'Y' represents the concrete mixture (A: Mix A or B: Mix B). Fig. 1 depicts the specimens' configurations and reinforcement details. Each specimen was 2.2 m in length and had a 150 × 260 mm cross-section. Since the study was rather focused on the effects of the stirrups' material (i.e. steel Vs. GFRP), the longitudinal reinforcement was kept the same for all beam specimens, consisting of 12 mm diameter steel bars at the bottom and 8 mm diameter steel bars used as top reinforcement. A 20-mm clear cover was maintained from all beam sides, making an effective depth (d) of 221 mm. As for transverse reinforcement, double-leg stirrups of 8 mm in diameter were placed at 200 mm spacing, and the CSS stirrups were varied among the test specimens as shown in Table 2. The yield stress of the 8 mm and 12 mm steel reinforcement was measured as 313 and 594 MPa, respectively, with an approximate elastic modulus of 220 GPa. As per the manufacturer [61], the GFRP reinforcement had a guaranteed tensile strength of 760 MPa and a maximum strain of 1.7%, with a tensile modulus of 45 MPa.

2.3. Test setup and instrumentation

The test setup for a typical specimen is illustrated in Fig. 2. The specimens were tested under 3-point loading after 28 days following casting using an Instron 1500 HDX Static Hydraulic testing machine. Displacement-controlled load was applied at a rate of 0.25 mm/min until failure. Linear variable displacement transducers (LVDTs) were placed on both sides of the specimen at the loading point to monitor the vertical displacement (Fig. 2). A clip-type transducer was placed at a 45° angle to measure the shear crack width (Fig. 2). A 60 mm strain gage was glued to the top surface of the specimens to measure the concrete compressive strains (as shown in Fig. 1-a). The tensile strains of the longitudinal and transverse reinforcements were measured using 5 mm strain gages placed at locations shown in Fig. 1-a. The strain gages were installed on two particular CSS stirrups (named here as the inner and middle stirrups according to their location from the loading point as shown in Fig. 1-a). A data acquisition system was used to capture the readings at a frequency of 1 Hz.

3. Experimental results

3.1. Modes of failure

Column 10 of Table 3 lists the failure modes of the tested specimens.

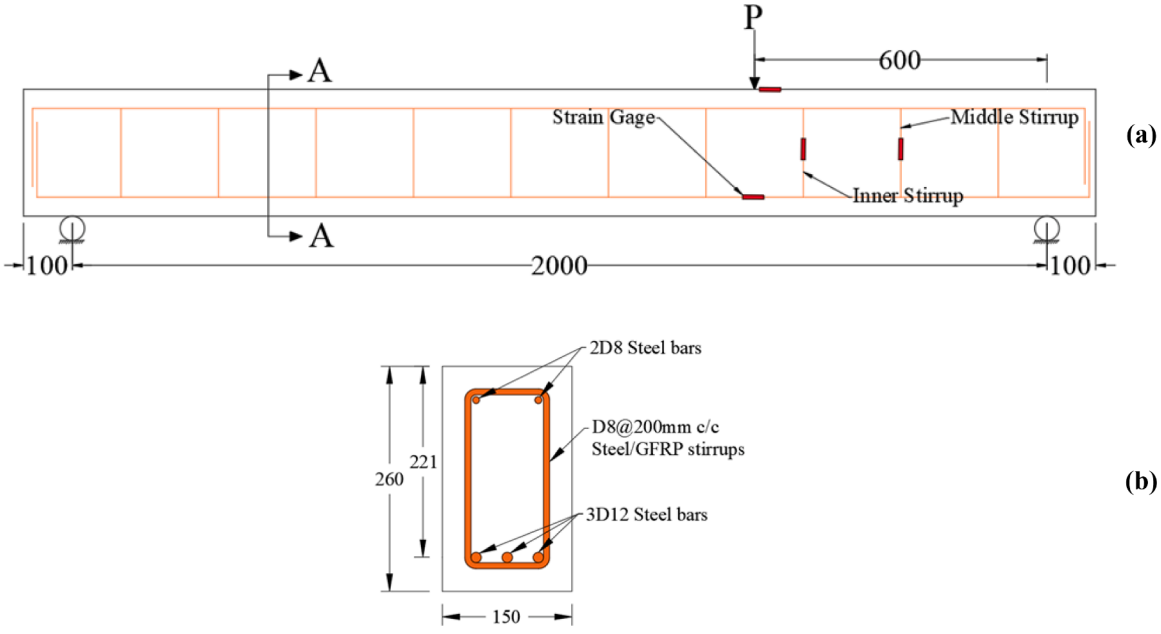

Fig. 1. Schematic drawing for a typical RC beam— (a) specimen's configuration; (b) reinforcement details.

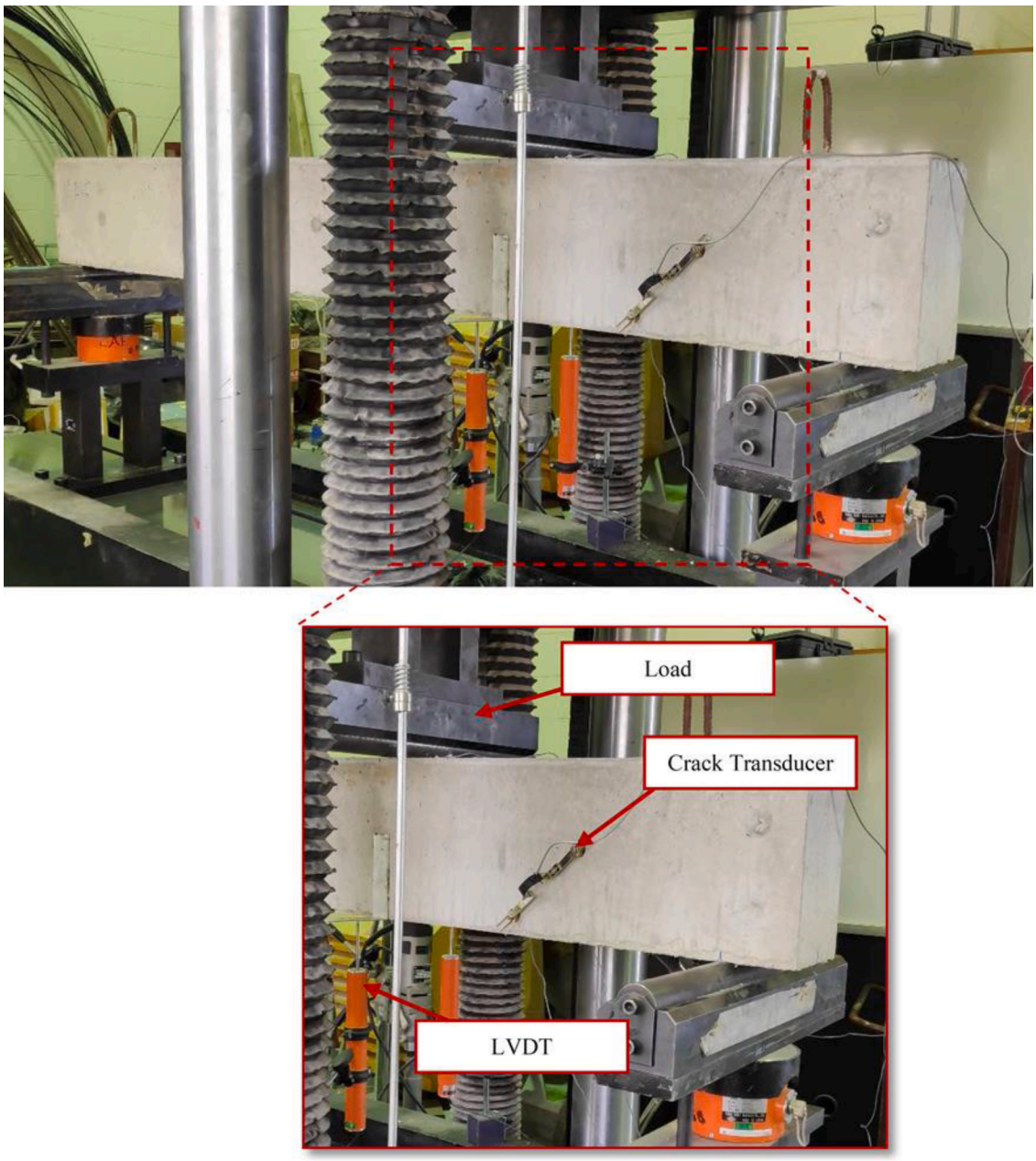

Fig. 2. Test setup and instrumentation.

Table 3
Summary of the experimental results.

1 Specimen	2 P_u(kN)	3 δ_u (mm)	4 $\varepsilon_{c,max}(\mu\varepsilon)$	5 $\varepsilon_{l,u}(\mu\varepsilon)$	6 $\varepsilon_{vm,u}(\mu\varepsilon)$	7 $\varepsilon_{vi,u}(\mu\varepsilon)$	8 ψ (kN.mm)	9 w_{max} (mm)	10 Failure Mode*
N-A	73.8	4.6	1084	2352	–	–	208	2.9	S
N-B	64.2	3.8	819	1683	–	–	150	2.7	S
S-A	101.2	15.0	2533	5220	2378	673	1177	3.3	$S+F$
S-B	89.7	8.1	3755	5276	2021	739	483	3.0	$S+F$
G-A	98.8	16.2	2279	4195	5933	3185	1237	5.7	$S+F$
G-B	89.7	8.0	1094	3164	3475	613	476	3.3	S

* S: shear failure; $S+F$: combined shear/flexural failure.

Two types of failure were observed, namely, shear failure (see Figs. 3-a, 3-b, and 3-f) and combined shear/flexural failure (see Figs. 3-c, 3-d, and 3-e). The shear failure started with the development of vertical cracks at the beam soffit due to flexural tensile stresses. After that, with increasing the load, one major crack extended and bended in a diagonal direction and moved to the upper surface of the beam toward the loading point as shown in Fig. 3-f (i.e. diagonal tension crack). This failure was accompanied by relatively low values of longitudinal strains at the concrete top surface and the rebars in tension (Columns 4 and 5, respectively). The combined shear/flexural failure was also characterized by a major

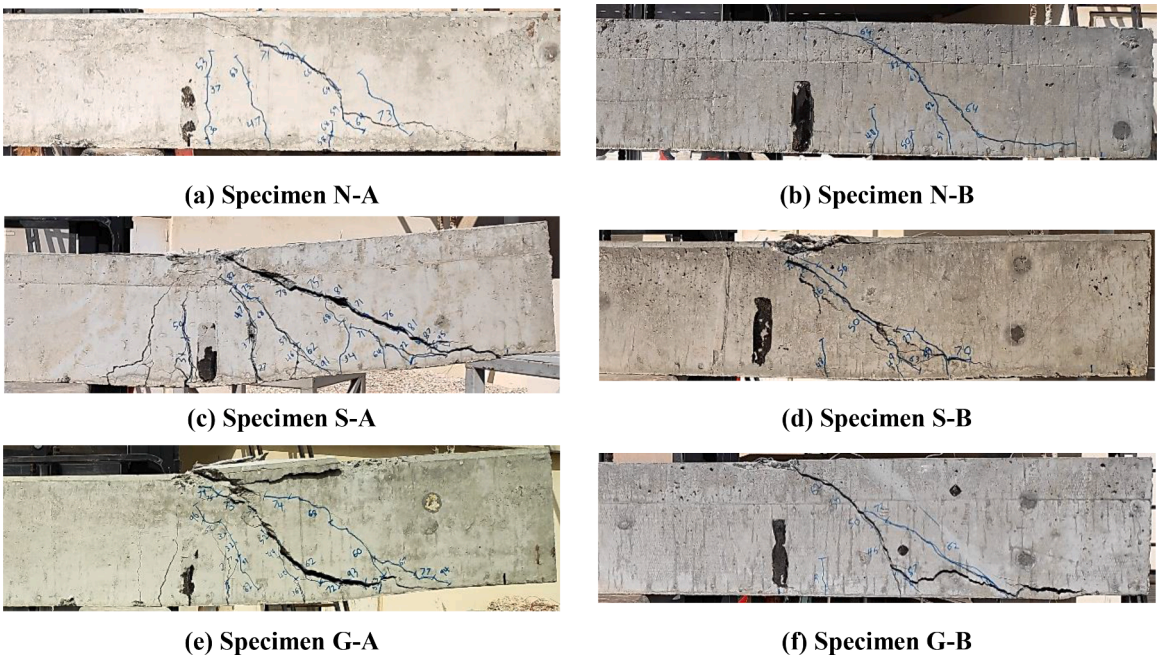

Fig. 3. Failure modes of the tested specimens.

diagonal-tension crack that extends between the loading point and the beam soffit. However, this failure was accompanied by additional flexural cracks and/or concrete crushing at the top (Fig. 3-e), in addition to relatively higher values of concrete and rebar strains (Columns 4 and 5, respectively). It is to be noted that Fig. 3 highlights that a significant interaction actually exists between the bending moment and the shear strength. This was corroborated by other shear-strength models proposed in the literature, that account for the variation of shear stresses along the depth of the beam at failure due to the interaction with bending (e.g. the variable strut inclination method with multiple strut inclinations [52], and the compression chord capacity model [62]).

As expected, beams without stirrups exhibited a shear failure, while those with steel/GFRP stirrups showed a combined shear/flexural failure due to the added shear resistance from the transverse reinforcement (Column 10 of Table 3). An exception to this rule was Specimen G-B which prematurely failed in shear. Apparently, combining RCA and GFRP in Specimen G-B had weakened the bond between GFRP stirrups and concrete, resulting in a fragile load transfer to stirrups and leading to premature shear failure in concrete. This can be observed from the low dowel action and horizontal splitting cracks in GFRP-RC beams (see Fig. 3-e) that somewhat indicate a reduced concrete/reinforcement bond. Such observations were corroborated by previous studies that indicate a reduced concrete/rebar bond associated with the use of RCA [63] or GFRP reinforcement [64].

3.2. Load-carrying capacity

The load-carrying capacity (P_u) for each specimen is presented in Column 2 of Table 3. In general, Mix A specimens exhibited higher P_u values compared to their Mix B counterparts (by 12% on average), consistent with previous studies on the shear strength of recycled-aggregate concrete beams [20,22,23,30]. This behavior was because the shear force in Mix A specimens was partially resisted by the aggregate interlock [28], and the shear cracks developed around the aggregate as shown in Fig. 4-a. On the other hand, Mix B specimens showed lower P_u values because of the RCA high porosity, the presence of

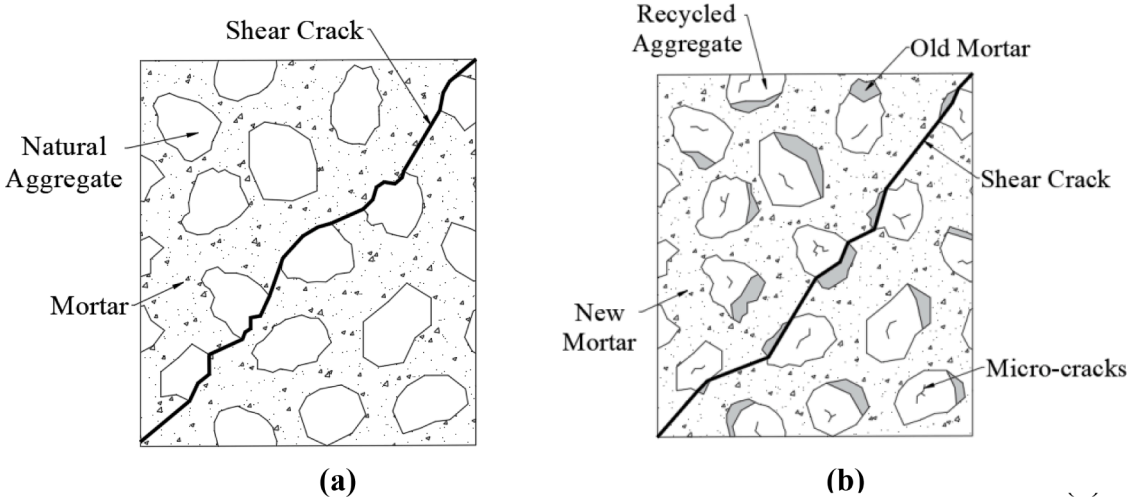

Fig. 4. Development of shear crack in (a) natural-aggregate and (b) recycled-aggregate concrete beams.

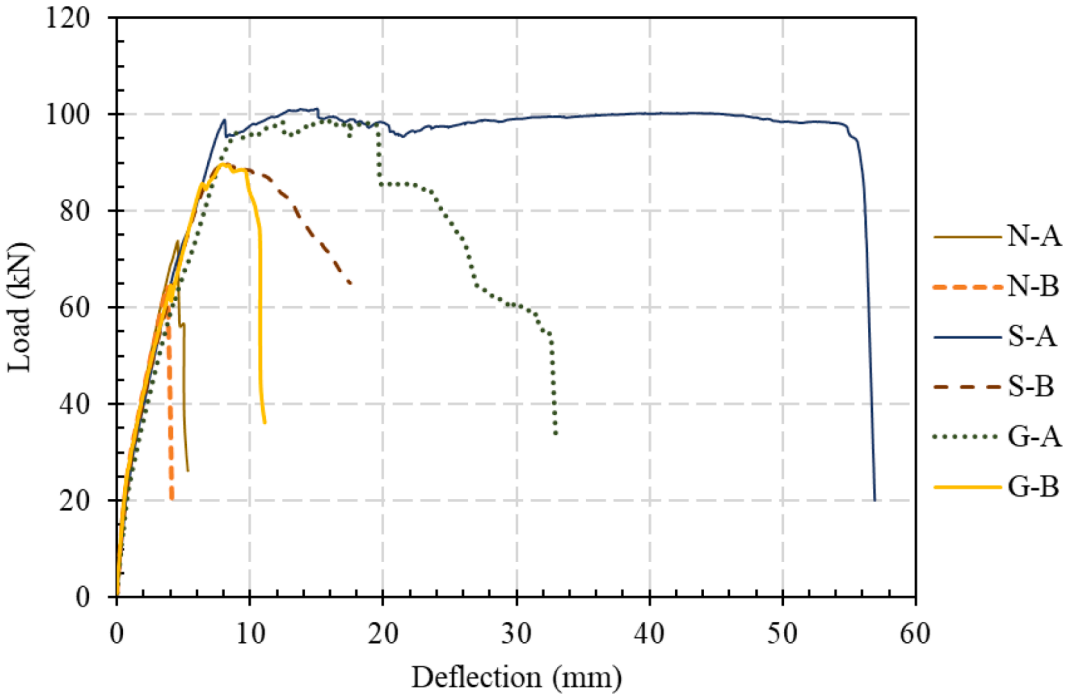

Fig. 5. Load vs. deflection diagrams for the tested specimens.

micro-cracks within the RCA, and the weak dual interfacial transition zone normally existing in recycled-aggregate concrete (viz. coarse aggregate/old mortar and RCA/new mortar interfaces) [65]. Consequently, the shear cracks broke through the RCA as shown in Fig. 4-b [28]. As for reinforcement material, specimens with steel and GFRP stirrups showed increases in P_u values by 38% and 37% on average, respectively, compared to their counterparts with no stirrups. The difference in the shear strength between the test specimens with GFRP versus steel stirrups having the same diameters and spacings was not significant ($\leq$ 5%); this somewhat conforms with previous studies on GFRP-RC beams [39,47].

3.3. Deformational characteristics

Fig. 5 depicts the load-deflection relationship for the tested specimens, and Column 3 of Table 3 lists the deflection measured at ultimate load (δ_u). Specimens with steel stirrups showed higher ductility performance compared to those with GFRP stirrups, attributable to the brittle behavior of GFRP. This is demonstrated by comparing the load-deflection diagrams between Specimens S-A and G-A (Fig. 5): the ductility index (defined here as the ratio between deflection at failure to that at longitudinal steel yielding) was measured as 6.4 for the former and 2.2 for the latter. Furthermore, Mix A specimens showed more ductile behavior compared to Mix B specimens (Fig. 5). The superior ductility of Mix A specimens is attributed to the stronger bond between the natural-aggregate concrete and the longitudinal reinforcement as compared to that provided by recycled-aggregate concrete in Mix B specimens [63,66]. This is further demonstrated by comparing the load-deflection diagrams between Specimens G-A and G-B: the former shows a post-P_u plateau, whereas the latter shows a sudden drop at P_u.

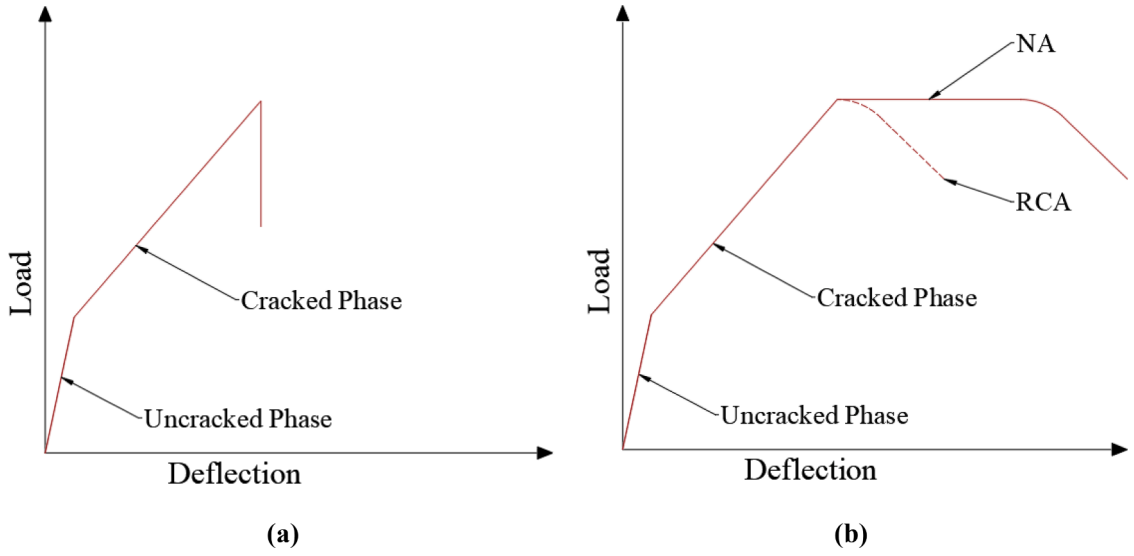

Fig. 6. Idealization of load–deflection relationship for (a) shear failure and (b) combined shear/flexural failure.

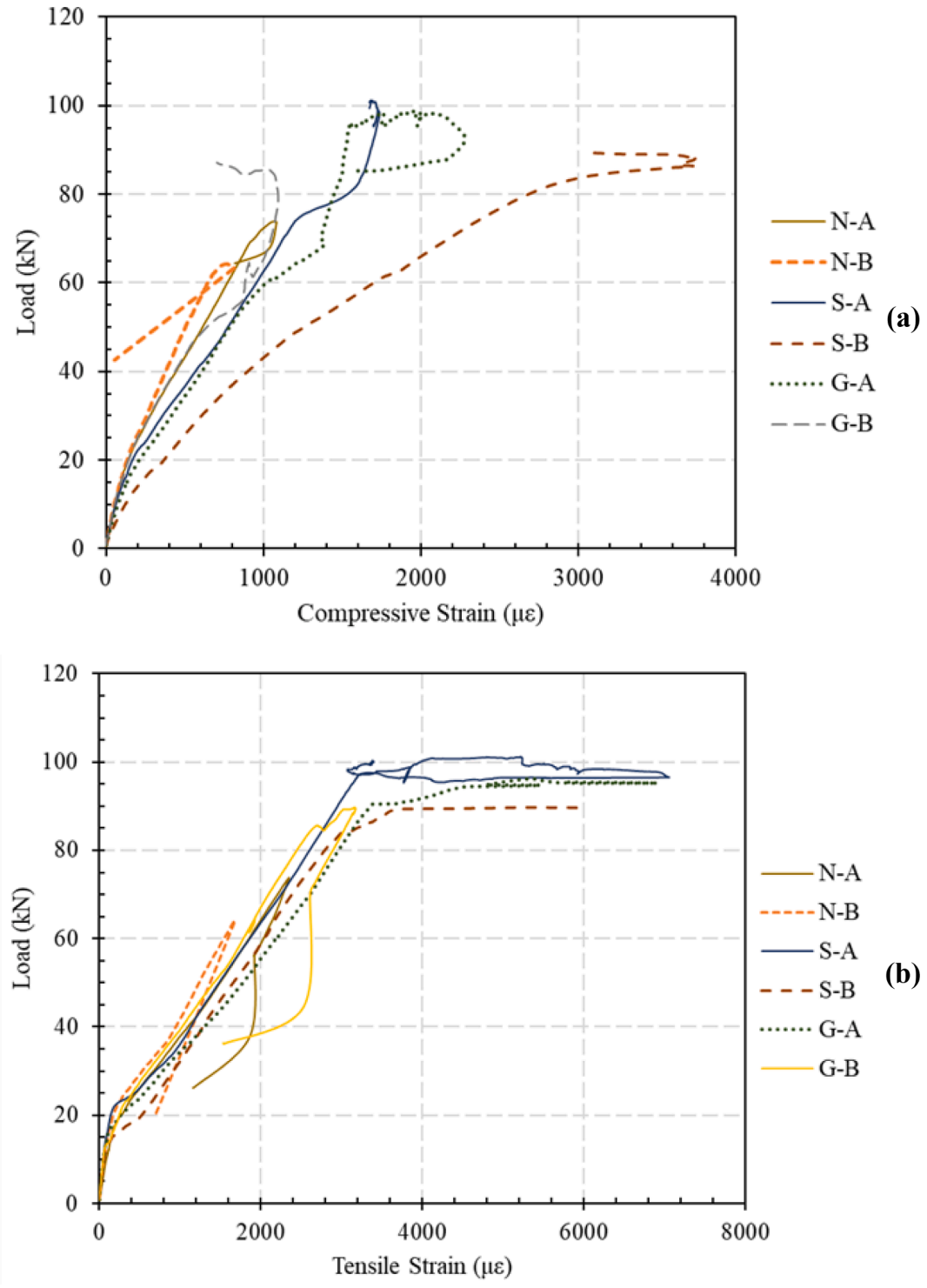

Fig. 7. Longitudinal strain measurements— (a) concrete compressive strain; (b) rebar tensile strain.

The concrete mixture showed little-to-no effect on the deformational characteristics of RC beams without stirrups.

The load-deflection diagrams of the tested specimens (Fig. 5) were consistent with the observed failure modes (Column 10 of Table 3). Fig. 6 presents an idealization of the load-deflection diagrams for the tested specimens based on their corresponding failure behavior. A sudden/steep decline at the P_u point was observed in the case of beams that had a shear failure (see Specimens N-A, N-B, and G-B in Fig. 5; idealized in Fig. 6-a). In contrast, an extended plateau following P_u point was noticed in the beams that exhibited a combined shear/flexural failure (see Specimens S-A, S-B, and G-A in Fig. 5; idealized in Fig. 6-b). However, this plateau showed an early and gradual decline in the case of using RCA (see Specimen S-B in Fig. 5) and so, this particular beam leaned more towards the shear side of the failure.

3.4. Strain characteristics

The maximum concrete compressive strain ($\varepsilon_{c,max}$) as well as rebar tensile strain at ultimate load ($\varepsilon_{l,u}$) are reported in Columns 4 and 5 of Table 3, respectively. Figs. 7-a and 7-b plot the load-concrete strain (P –

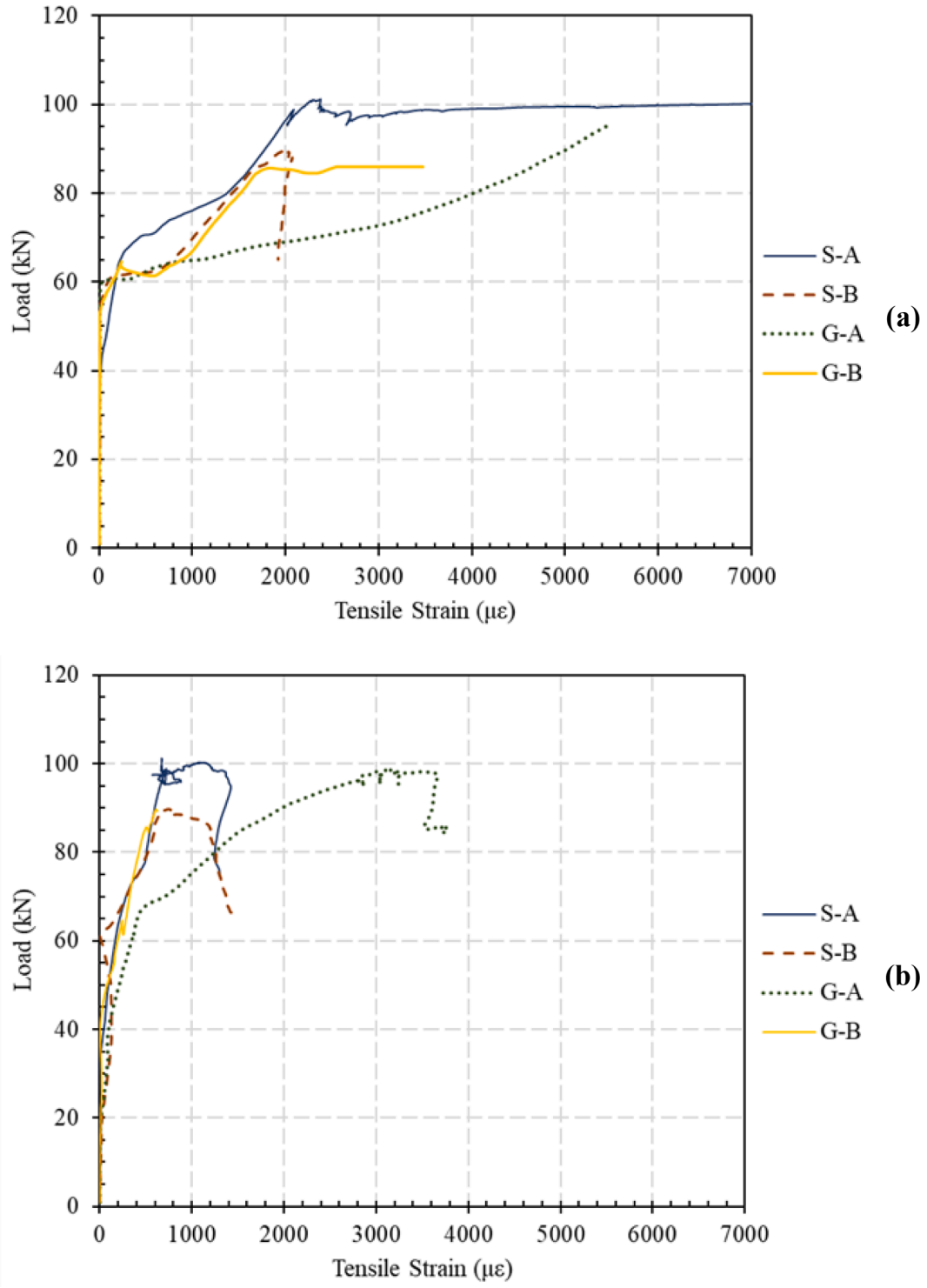

Fig. 8. Vertical strain measurements— (a) middle-stirrups tensile strain; (b) inner-stirrups tensile strain.

ε_c) and the load-rebar strain ($P - \varepsilon_l$) diagrams for the tested specimens, respectively. In general, the longitudinal strains conformed with the load-deflection diagrams and the failure behaviors of the tested specimens. The beams that failed due to combined shear/flexure showed higher $\varepsilon_{c,max}$ and $\varepsilon_{l,u}$ compared to those merely failing in shear. As expected, specimens without stirrups (N-A and N-B) exhibited lower $\varepsilon_{l,u}$ and $\varepsilon_{c,max}$ as compared to the specimens with steel/GFRP stirrups. In agreement with the observations on deformational characteristics (Section 3.3), specimens with steel stirrups and natural-aggregate concrete showed higher longitudinal strains (ε_c and ε_l) compared to their recycled-aggregate GFRP-reinforced counterparts. Mix A specimens had 36% higher $\varepsilon_{l,u}$ values on average than those of their Mix B counterparts, mostly attributed to the weaker bond between longitudinal steel and recycled-aggregate concrete [63,66]. Comparing $P - \varepsilon_l$ diagrams between Specimens G-A and G-B in particular (Fig. 7-b), the post-P_u curve was missing in the latter as this specimen prematurely failed in shear.

As for vertical strains, the middle stirrup strain ($\varepsilon_{vm,u}$) and the inner stirrup strain ($\varepsilon_{vi,u}$) measured at P_u are presented in Columns 6 and 7 of Table 3, respectively. Figs. 8-a and 8-b depict the $P - \varepsilon_{vm}$ and $P - \varepsilon_{vi}$ diagrams for the tested specimens, respectively. The middle stirrups had

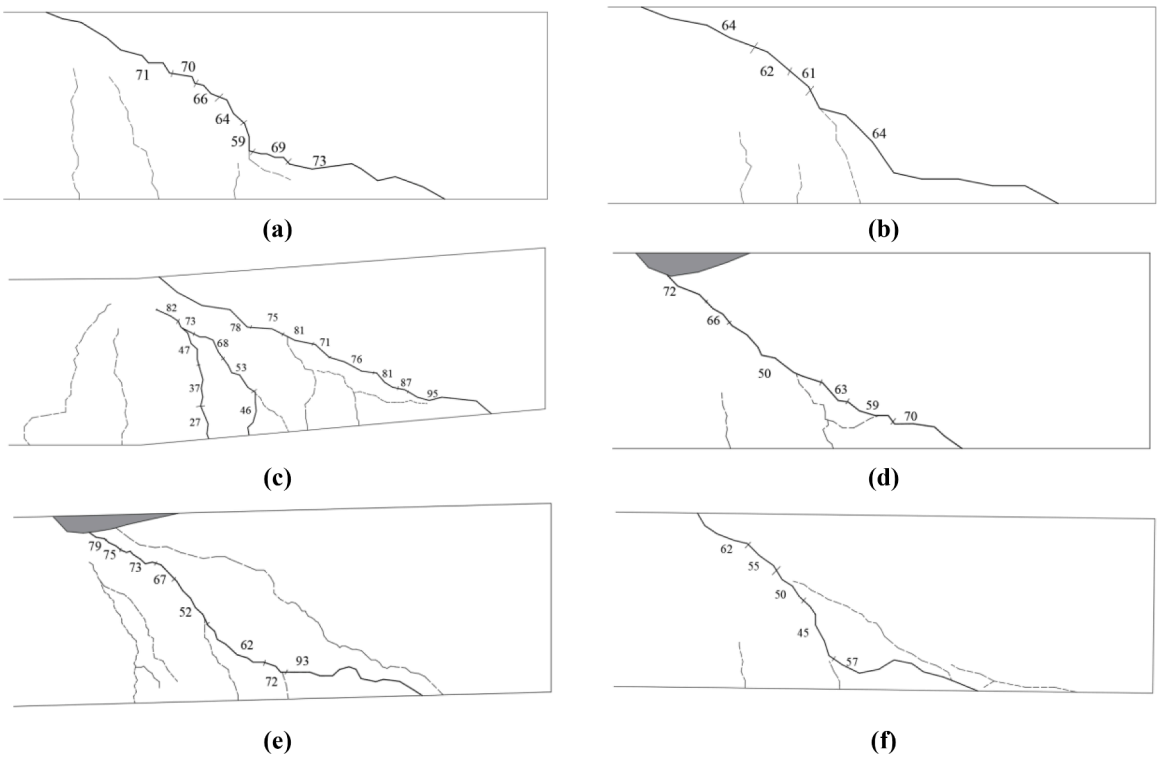

Fig. 9. Cracking patterns for (a) N-A, (b) N-B, (c) S-A, (d) S-B, (e) G-A, and (f) G-B.

significantly higher strain values compared to the inner stirrups, as the former lied within a critical zone (i.e. in the middle of the strut) where, in theory, internal shear forces and cracks are maximized [67]. On average, the $\varepsilon_{vm,u}$ values for Mix A specimens were 45% higher than that of their Mix B counterparts. This can be attributed to the higher P_u reached by Mix A specimens as well as the enhanced bond between concrete and stirrups [63,66]. Specimens with steel stirrups showed approximately 50% lower $\varepsilon_{vm,u}$ compared to those with GFRP stirrups, on average. This is attributed to the higher elastic modulus of steel (220 GPa) compared to that of GFRP (45 GPa), that allowed the steel to resist high loads at lower strains.

3.5. Energy absorption

Energy absorption (ψ) refers to the area under the load-deflection curve and it is an indication of the structural performance [68]. The ψ

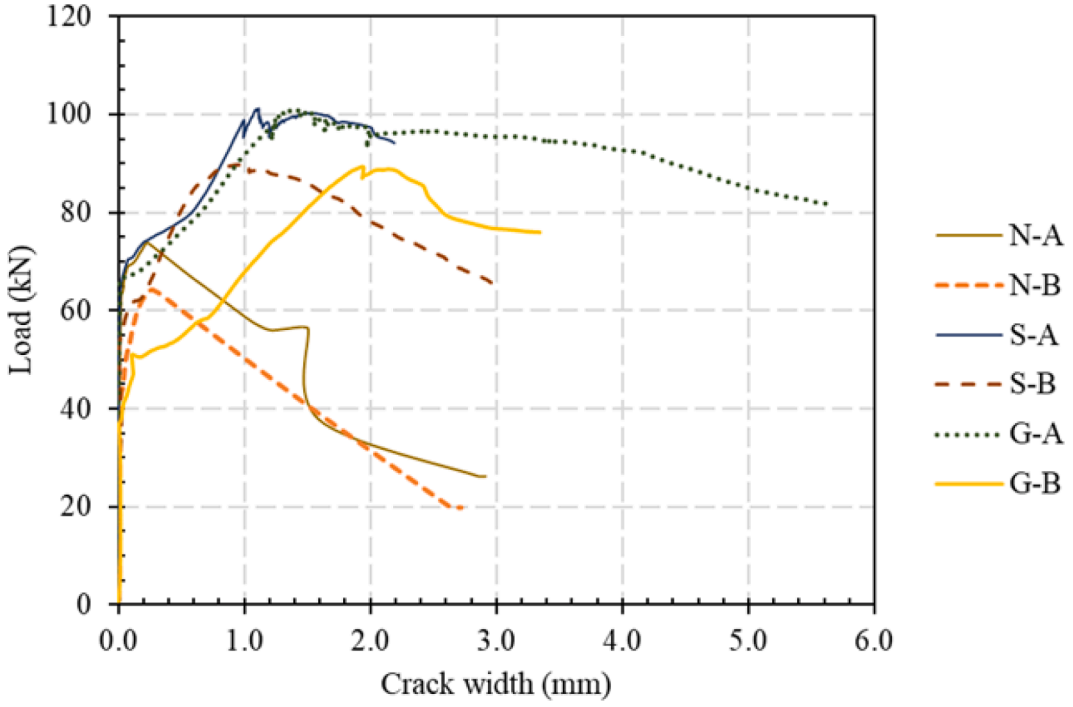

Fig. 10. Load vs. crack-width diagrams for the tested specimens.

values obtained for the tested beams are listed in Column 8 of Table 3. Indeed, the absence of C.S.S. stirrups (in Specimens N-A and N-B) led to a significant reduction in ψ (by 75% on average) as a result of reduced deformations and load-carrying capacities. The effect of the stirrups' material (steel or GFRP) was insignificant, though, on the energy absorption. As for the effect of the concrete mixture, the average ψ values for Mix A and Mix B specimens were 874 and 370 kN.mm, respectively. The advantage of Mix A over Mix B specimens in terms of energy absorption is attributed to their higher load-carrying capacity as well as superior ductility performance (as discussed in Section 3.3).

3.6. Cracking behavior

The cracking patterns of the tested specimens are sketched in Fig. 9. The major and minor cracks are expressed as solid and dashed lines, respectively, while the gray/shaded area represents concrete crushing. The number of cracks was generally higher in specimens with a combined shear/flexural failure compared to those failing in shear, owing to the higher ductility and load-carrying capacity of the former. As for concrete mixtures, Mix A specimens showed a greater number of cracks compared to their Mix B counterparts, despite having similar failure modes. This can be demonstrated by comparing the cracking patterns between Specimens N-A (Fig. 9-a) and N-B (Fig. 9-b) as well as Specimens S-A (Fig. 9-c) and S-B (Fig. 9-d). The stirrups material (GFRP or steel) had insignificant effects on the cracking pattern.

Column 9 of Table 3 lists the maximum crack width (w_{max}) values for the tested beams. Specimens without stirrups showed a reduced w_{max} (by ~25% on average): this is because the provision of steel/GFRP stirrups increased P_u, promoted the beam's ductility, and thus led to an increased w_{max} at failure. As for concrete mixtures, Mix B specimens showed slightly lower w_{max} values as compared to their Mix A counterparts, mostly due to their lower load-carrying capacities that led to less acute cracks at failure. However, during the loading stage (i.e. before failure), Mix B specimens showed higher w values, especially in the case of using GFRP stirrups. For instance, at 80-kN load level, the reported crack width of Specimen G-B (1.48 mm) was higher than that of Specimen G-A (0.66 mm).

Indeed, the failure mode had reflected on the specimens' crack width. For instance, Specimen G-B had a lower w_{max} (by ~40%) compared to its counterpart (Specimen G-A) as the former prematurely failed in shear. Using GFRP stirrups in place of steel led to an average increase of 40% in w_{max}, mostly because of the higher tensile strains of GFRP stirrups compared to steel (owing to their lower elastic modulus as discussed in Section 3.4). Likewise, the load versus crack width diagrams of the tested specimens (Fig. 10) were consistent with their failure modes and deformational characteristics. As shown in Fig. 10, the $P-w$ curve suddenly drops at P_u for the specimens that had failed in shear, while it gradually declines following P_u point for the specimens with a combined shear/flexural failure.

4. Theoretical formulations

The nominal shear resistance (V_n) is the sum of the concrete contribution (V_c) and the stirrups contribution (V_s for steel or V_f for FRP) as per Eq. (1). Based on the force equilibrium of the beam shown in Fig. 1-a, the theoretical load-carrying capacity (P_{u-th}) can be estimated as $P_{u-Th} = 1.43V_n$.

$$V_n = V_c + V_{s\ or\ f} \tag{1}$$

The P_{u-Th} was estimated using four commonly-used design guides for steel/GFRP RC design, namely, ACI [34,69], CSA [35,70], EC2 [36], and ISIS [71]. To facilitate the comparison between the different codes, the inclination angle of the diagonal compressive strut (θ) was uniformly taken as 45°.

In accordance with ACI 318M-14 [34], the V_c and V_s contributions were calculated as follows:

$$V_c = \left(0.16\sqrt{f'_c} + 17\rho_w\right)bd \tag{2a}$$

$$V_s = \frac{A_v f_{yt} d}{s} \tag{2b}$$

where f'_c is the 28-day compressive strength of concrete (Table 1), ρ_w is the reinforcement ratio (0.01), b is the beam width (150 mm), d is the effective depth of the longitudinal reinforcement (221 mm), A_v is the area of shear reinforcement (100 mm^2) within the spacing s (200 mm), and f_{yt} is the stirrups yield stress (313 MPa). As for the GFRP stirrups, ACI 440.1R-15 [69] provisions were used, and the GFRP contribution (V_f) was calculated as per Eq. (2b) considering the GFRP tensile parameters ($E_f = 45GPa$ and $f_{fv} = f^*_{fu} = 760\ MPa$).

The simplified method was used as per CSA A23.3–04 [35] to calculate V_c and V_s, as follows:

$$V_c = \beta\sqrt{f'_c}bd_v \tag{3a}$$

$$V_s = \frac{A_v f_{yt} d_v \cot\theta}{s} \tag{3b}$$

where β was taken as 0.18 for specimens with stirrups and as $\frac{230}{2000+d_v}$ for specimens without stirrups, and d_v is the effective depth of the shear-critical beam (taken as $0.9d$). As for GFRP stirrups, the V_f was calculated according to CSA S806–12 [70], as follows:

$$V_f = \frac{0.4A_v f_{fu} d_v \cot\theta}{s} \tag{4}$$

The Euro code EC2 [36] was used to calculate the shear strength only for specimens without stirrups or those with CSS steel stirrups. The V_c and V_s contributions were obtained as per Eq. (5), as follows:

$$V_c = C_{rd}k\left(100\rho_s f'_c\right)^{\frac{1}{3}}bd \tag{5a}$$

$$V_s = \frac{A_v f_{yt} d_v \cot\theta}{s} \tag{5b}$$

$$k = 1 + \sqrt{\frac{200}{d}} \le 2 \tag{5c}$$

where C_{rd} was taken as 0.18 as recommended by the code. In principle, EC2 [36] neglects the concrete contribution (V_c) while allowing θ to be considered as low as 21.8°, which usually leads to very conservative results [53]. Here, as formerly indicated, we considered θ = 45° while simultaneously accounting for the concrete contribution, to allow for a valid comparison among the design guides.

The ISIS design guide [71] was used to calculate the shear strength only for specimens with GFRP/no stirrups. The V_c and V_f contributions were calculated as follows:

$$V_c = 0.2\sqrt{f'_c}bd \tag{6a}$$

$$V_f = \frac{A_v \sigma_v d_v \cot\theta}{s} \tag{6b}$$

$$\sigma_v = \frac{\left(0.05\frac{r_b}{d_b} + 0.3\right)f_{Fu}}{1.5} \tag{6c}$$

where r_b is the bend radius for GFRP stirrups and d_b is the bar diameter (the $\frac{r_b}{d_b}$ ratio was considered as 3).

Table 4 presents a comparison between theoretical (P_{u-th}) and experimental (P_u) load-carrying capacities for the tested specimens. Indeed, as f'_c was nearly the same between Mix A and Mix B concretes,

Table 4
Comparison of experimental and theoretical predictions.

Method	N-A		N-B		S-A		S-B		G-A		G-B	
Experimental	73.8		64.2		101.2		89.7		98.8		89.7	
ACI [34,69]	60.4	(1.22)	59.4	(1.08)	110.1	(0.92)	109.1	(0.82)	88.8	(1.11)	87.8	(1.02)
CSA [35,70]	56.5	(1.31)	55.4	(1.16)	97.7	(1.04)	96.7	(0.93)	96.4	(1.02)	95.4	(0.94)
EC2 [36]	60.8	(1.21)	60.0	(1.07)	105.4	(0.96)	104.7	(0.86)	–	–	–	–
ISIS Module 3 [71]	65.4	(1.13)	64.2	(1.00)	–	–	–	–	97.9	(1.01)	96.8	(0.93)

The ratio $\frac{P_u}{P_{u-Th}}$ is provided between parentheses.

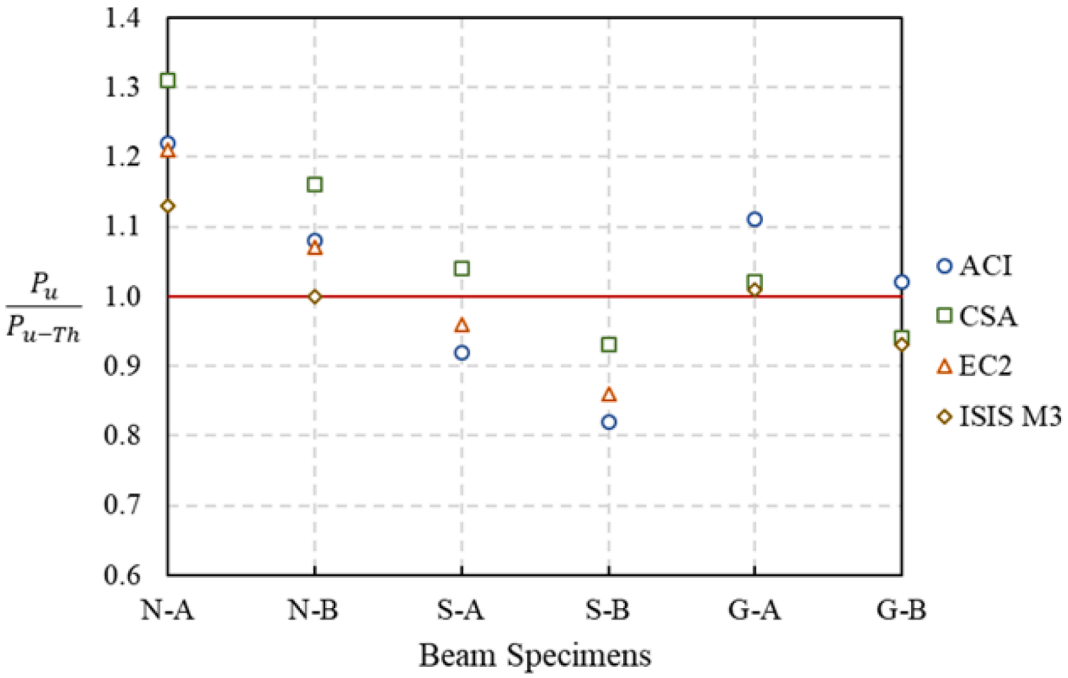

Fig. 11. Comparison between experimental results and theoretical formulations.

the P_{u_Th} values of their corresponding specimens were comparable. In general, we obtained a reasonable agreement between the experimental and theoretical values of P_u for the tested specimens. The average difference between P_{u_th} and P_u values was measured for each design guide as 11.6% for ACI [34,69], 11.0% for CSA [35,70], 11.7% for EC2 [36], and 5.3% for ISIS [71], overall making 10% difference on average. Fig. 11 portrays a comparison among the design guides in terms of shear strength prediction. Among the design guides used here, the CSA codes [35,70] produced the most conservative results, and the predictions of the ISIS design guide [71] were the closest to the experimental P_u values. The design guides were observed to be most conservative in case no stirrups are provided. Furthermore, the design guides generally overestimated the shear strength in the case of using recycled-aggregate concrete beams with steel or GFRP stirrups.

5. Summary and conclusions

This paper investigated the shear behavior of recycled-aggregate concrete beams with GFRP stirrups. Six RC beam specimens were tested under three-point loading considering two test variables, namely, aggregate type (natural/recycled) and shear reinforcement (none/conventional steel/GFRP). Based on the results of this study, we conclude the following:

- Two modes of failure were observed, namely, shear failure and combined shear/flexural failure: the failure in RC beams generally leaned towards the former when using RCA in the concrete mix. The cracking pattern was generally comparable among the beam specimens; however, those with GFRP stirrups showed higher crack widths due to the relatively weak concrete/GFRP bond as well as the GFRP lower stiffness.
- Using recycled coarse aggregate in concrete reduced the shear strength of RC beams by 12% on average, even though the concrete strength was preserved by adjusting the mixture design. The effects of using GFRP stirrups in place of steel stirrups were not significant, though, on the load-carrying capacity ($\leq$ 2%).
- Beams with steel stirrups exhibited higher ductility performance than those with GFRP stirrups, which can be attributed to the inherent brittle behavior of GFRP. Similarly, natural-aggregate concrete beams showed more ductile behavior compared to their recycled-aggregate counterparts, thanks to the relatively strong bond between natural-aggregate concrete and the reinforcement bars/stirrups.
- Theoretically-predicted values of the shear strength were obtained for the tested beams based on contemporary design guides and compared with the experimental results. The predicted and the experimental values of the shear strength were in a reasonable agreement (with a 10% difference on average). The design guides were observed to be most conservative in case no stirrups are provided. Among the design guides used here, the CSA code produced the most conservative results, and the ISIS design guide was the most representative of the experimental results.

The above conclusions and especially the numbers are solely based on the materials and specimens used herein. While initial observations can only be made based on the limited number of specimens in the current study (only one specimen for each category is analyzed), future research is recommended to corroborate the findings reported here and to investigate other parameters such as longitudinal reinforcement, span-to-depth ratio, RCA replacement level, etc.

Data availability statement

The data that support the findings of this study are available on request from the corresponding author.

Declaration of Competing Interest

The authors declare that they have no known competing financial interests or personal relationships that could have appeared to influence the work reported in this paper.

Acknowledgement

This effort was made possible by the NPRP Grant # NPRP13S-0209–200311 from Qatar National Research Fund (a member of Qatar Foundation). The findings achieved herein are solely the responsibility of the authors. Heartfelt gratitude is owed to ATP Construction Composites and Readymix Qatar (as part of LafargeHolcim) for their help in preparing the test specimens.

References

[1] P.J.M. Monteiro, S.A. Miller, Towards sustainable concrete, Nat. Mater. 16 (2017) 698–699.
[2] Heede P.V., De Belie N. Environmental impact and life cycle assessment (LCA) of traditional and “green” concretes: literature review and theoretical calculations. Cement and concrete composites 2012;34:431–42. https://doi.org/10.1016/j.cemconcomp.2012.01.004.
[3] S.A. Miller, V.M. John, S.A. Pacca, A. Horvath, Carbon dioxide reduction potential in the global cement industry by 2050, Cem. Concr. Res. 114 (2017) 115–124, https://doi.org/10.1016/j.cemconres.2017.08.026.
[4] V.W.Y. Tam, M. Soomro, A.C.J. Evangelista, A review of recycled aggregate in concrete applications (2000–2017), Constr. Build. Mater. 172 (2018) 272–292, https://doi.org/10.1016/j.conbuildmat.2018.03.240.
[5] K. Rahal, Mechanical properties of concrete with recycled coarse aggregate, Build. Environ. 42 (2007) 407–415, https://doi.org/10.1016/j.buildenv.2005.07.033.
[6] Koch G., Varney J., Thompson N., Moghissi O., Gould M., Payer J. International measures of prevention, application, and economics of corrosion technologies study (IMPACT). 2016.
[7] L.N. Koutas, Z. Tetta, D.A. Bournas, T.C. Triantafillou, Strengthening of concrete structures with textile reinforced mortars : state-of-the-art review, J. Compos. Constr. 23 (2019), 03118001, https://doi.org/10.1061/(ASCE)CC.1943-5614.0000882.
[8] A.B.M.A. Kaish, M. Jamil, S.N. Raman, M.F.M. Zain, L. Nahar, Ferrocement composites for strengthening of concrete columns: a review, Constr. Build. Mater. 160 (2018) 326–340, https://doi.org/10.1016/j.conbuildmat.2017.11.054.
[9] A. Parghi, M.S. Alam, A review on the application of sprayed-FRP composites for strengthening of concrete and masonry structures in the construction sector, Compos. Struct. 187 (2018) 518–534, https://doi.org/10.1016/j.compstruct.2017.11.085.
[10] Z. Wu, X. Wang, X. Zhao, M. Noori, State-of-the-art review of FRP composites for major construction with high performance and longevity, Int. J. Sustainable Mater. Structural Sys. 1 (2014) 201, https://doi.org/10.1504/IJSMSS.2014.062757.
[11] D’Antino T., Pisani M.A. Long-term behavior of GFRP reinforcing bars. Composite Structures 2019:111283. https://doi.org/10.1016/j.compstruct.2019.111283.
[12] X. Shan, J. Zhou, V.W.C. Chang, E.H. Yang, Life cycle assessment of adoption of local recycled aggregates and green concrete in Singapore perspective, J. Clean. Prod. 164 (2017) 918–926, https://doi.org/10.1016/j.jclepro.2017.07.015.
[13] Hossain M.U., Poon C.S., Lo I.M.C., Cheng J.C.P. Comparative environmental evaluation of aggregate production from recycled waste materials and virgin sources by LCA. Resources, conservation and recycling 2016;109:67–77. https://doi.org/10.1016/j.resconrec.2016.02.009.
[14] S. Butera, T.H. Christensen, T.F. Astrup, Life cycle assessment of construction and demolition waste management, Waste Manage. (Oxford) 44 (2015) 196–205, https://doi.org/10.1016/j.wasman.2015.07.011.
[15] T. Cadenazzi, G. Dotelli, M. Rossini, S. Nolan, A. Nanni, Life-cycle cost and life-cycle assessment analysis at the design stage of a fiber-reinforced polymer-reinforced concrete bridge in Florida, Adv. Civil Eng. Mater. 8 (2019), 20180113, https://doi.org/10.1520/ACEM20180113.
[16] C. Zhang, Life cycle assessment (LCA) of fibre reinforced polymer (FRP) composites in civil applications. eco-efficient construction and building materials: life Cycle Assessment (LCA), eco-labelling and case studies, Woodhead Publishing Limited (2014) 565–591, https://doi.org/10.1533/9780857097729.3.565.
[17] T. Cadenazzi, G. Dotelli, M. Rossini, S. Nolan, A. Nanni, Cost and environmental analyses of reinforcement alternatives for a concrete bridge, Struct. Infrastruct. Eng. (2019) 1–16, https://doi.org/10.1080/15732479.2019.1662066.
[18] A. Younis, U. Ebead, P. Suraneni, A. Nanni, Cost effectiveness of reinforcement alternatives for a concrete water chlorination tank, J. Building Eng. 27 (2020), 100992, https://doi.org/10.1016/j.jobe.2019.100992.
[19] A. Younis, U. Ebead, S. Judd, Life cycle cost analysis of structural concrete using seawater, recycled concrete aggregate, and GFRP reinforcement, Constr. Build. Mater. 175 (2018) 152–160, https://doi.org/10.1016/j.conbuildmat.2018.04.183.
[20] E. Alrajfi, A.M. Ashteyat, Y.Z. Murad, Shear behaviour of RC beams made with natural, recycled aggregate concrete and reclaimed asphalt aggregates under normal and elevated temperature, J. Building Eng. 40 (2021), 102681, https://doi.org/10.1016/j.jobe.2021.102681.
[21] H. Ju, M. Yerzhanov, A. Serik, D. Lee, J.R. Kim, Statistical and reliability study on shear strength of recycled coarse aggregate reinforced concrete beams, Materials (Basel) 14 (2021) 3321, https://doi.org/10.3390/ma14123321.
[22] M. Setkit, S. Leelatanon, T. Imjai, R. Garcia, S. Limkatanyu, Prediction of shear strength of reinforced recycled aggregate concrete beams without stirrups, Buildings 11 (2021) 402, https://doi.org/10.3390/buildings11090402.
[23] H.B. Choi, C.K. Yi, H.H. Cho, K.I. Kang, Experimental study on the shear strength of recycled aggregate concrete beams, Mag. Concr. Res. 62 (2010) 103–114, https://doi.org/10.1680/macr.2008.62.2.103.
[24] I.S. Ignjatović, S.B. Marinković, N. Tošić, Shear behaviour of recycled aggregate concrete beams with and without shear reinforcement, Eng. Struct. 141 (2017) 386–401, https://doi.org/10.1016/j.engstruct.2017.03.026.
[25] S. Pradhan, S. Kumar, S.V. Barai, Shear performance of recycled aggregate concrete beams: an insight for design aspects, Constr. Build. Mater. 178 (2018) 593–611, https://doi.org/10.1016/j.conbuildmat.2018.05.022.
[26] A.M. Knaack, Y.C. Kurama, Behavior of reinforced concrete beams with recycled concrete coarse aggregates, J. Structural Eng. (United States) 141 (2015), B4014009, https://doi.org/10.1061/(ASCE)ST.1943-541X.0001118.
[27] K.N. Rahal, Y.T. Alrefaei, Shear strength of longitudinally reinforced recycled aggregate concrete beams, Eng. Struct. 145 (2017) 273–282, https://doi.org/10.1016/j.engstruct.2017.05.028.
[28] K.N. Rahal, Y.T. Alrefaei, Shear strength of recycled aggregate concrete beams containing stirrups, Constr. Build. Mater. 191 (2018) 866–876, https://doi.org/10.1016/j.conbuildmat.2018.10.023.
[29] J. Xiao, W. Li, Y. Fan, X. Huang, An overview of study on recycled aggregate concrete in China (1996–2011), Constr. Build. Mater. 31 (2012) 364–383, https://doi.org/10.1016/j.conbuildmat.2011.12.074.
[30] M. Arezoumandi, A. Smith, J.S. Volz, K.H. Khayat, An experimental study on shear strength of reinforced concrete beams with 100% recycled concrete aggregate, Constr. Build. Mater. 53 (2014) 612–620, https://doi.org/10.1016/j.conbuildmat.2013.12.019.
[31] K.N. Rahal, W. Hassan, Shear strength of plain concrete made of recycled low-strength concrete aggregates and natural aggregates, Constr. Build. Mater. 311 (2021), https://doi.org/10.1016/j.conbuildmat.2021.125317.
[32] D. De Domenico, F. Faleschini, C. Pellegrino, G. Ricciardi, Structural behavior of RC beams containing EAF slag as recycled aggregate: numerical versus experimental results, Constr. Build. Mater. 171 (2018) 321–337, https://doi.org/10.1016/j.conbuildmat.2018.03.128.
[33] K.N. Rahal, K. Elsayed, Shear strength of 50 MPa longitudinally reinforced concrete beams made with coarse aggregates from low strength recycled waste concrete, Constr. Build. Mater. 286 (2021), https://doi.org/10.1016/j.conbuildmat.2021.122835.
[34] ACI Committee 318. Building code requirements for structural concrete (ACI 318M-14) and commentary (ACI 318RM-14). 2014.
[35] Canadian Standards Association. CSA A23.3-04 Design of concrete structures. 2004.
[36] EN 1992-1-1 Eurocode 2: Design of Concrete Structures - Part 1-1: General ruels and Rules For Buildings, Comité Européen de Normalisation (CEN), Brussels, 2005.
[37] A.M. Ebid, A. Deifalla, Prediction of shear strength of FRP reinforced beams with and without stirrups using (GP) technique, Ain Shams Eng. J. 12 (2021) 2493–2510, https://doi.org/10.1016/j.asej.2021.02.006.
[38] A.G. Razaqpur, S. Spadea, Shear strength of FRP reinforced concrete members with stirrups, J. Compos. Constr. 19 (2015), https://doi.org/10.1061/(ASCE)CC.1943-5614.0000483.
[39] E.A. Ahmed, E.F. El-Salakawy, B. Benmokrane, Fibre-reinforced polymer composite shear reinforcement: performance evaluation in concrete beams and code prediction, Can. J. Civ. Eng. 37 (2010) 1057–1070, https://doi.org/10.1139/l10-046.
[40] K. Mahmoud, E. El-Salakawy, Shear strength of GFRP-reinforced concrete continuous beams with minimum transverse reinforcement, J. Compos. Constr. 18 (2014), 04013018, https://doi.org/10.1061/(ASCE)CC.1943-5614.0000406.
[41] L. Nguyen-Minh, M. Rovňák, Shear resistance of GFRP-reinforced concrete beams, Mag. Concr. Res. 63 (2011) 215–233, https://doi.org/10.1680/macr.9.00182.
[42] E.A. Ahmed, E.F. El-Salakawy, B. Benmokrane, Performance evaluation of glass fiber-reinforced polymer shear reinforcement for concrete beams, ACI Structural J. 107 (2010) 53–62, https://doi.org/10.14359/51663388.
[43] E.A. Ahmed, E.F. El-Salakawy, B. Benmokrane, Shear performance of RC Bridge girders reinforced with carbon FRP stirrups, J. Bridge Eng. 15 (2010) 44–54, https://doi.org/10.1061/(ASCE)BE.1943-5592.0000035.

[44] C. Lee, S. Lee, S. Shin, Shear capacity of RC beams with carbon fiber-reinforced polymer stirrups with rectangular section, J. Compos. Constr. 20 (2016), 04015085, https://doi.org/10.1061/(ASCE)CC.1943-5614.0000653.
[45] M. Said, M.A. Adam, A.A. Mahmoud, A.S. Shanour, Experimental and analytical shear evaluation of concrete beams reinforced with glass fiber reinforced polymers bars, Constr. Build. Mater. 102 (2016) 574–591, https://doi.org/10.1016/j.conbuildmat.2015.10.185.
[46] M.A. Issa, T. Ovitigala, M. Ibrahim, Shear behavior of basalt fiber reinforced concrete beams with and without basalt FRP stirrups, J. Compos. Constr. 20 (2016), 04015083, https://doi.org/10.1061/(ASCE)CC.1943-5614.0000638.
[47] E.C. Bentz, L. Massam, M.P. Collins, Shear strength of large concrete members with FRP reinforcement, J. Compos. Constr. 14 (2010) 637–646, https://doi.org/10.1061/(ASCE)CC.1943-5614.0000108.
[48] A. Al-Hamrani, W. Alnahhal, A Elahtem, Shear behavior of green concrete beams reinforced with basalt FRP bars and stirrups, Compos. Struct. 277 (2021), https://doi.org/10.1016/j.compstruct.2021.114619.
[49] Al-Hamrani A., Alnahhal W. Shear behavior of basalt FRC beams reinforced with basalt FRP bars and glass FRP stirrups: experimental and analytical investigations. Engineering Structures 2021;242. https://doi.org/10.1016/j.engstruct.2021.112612.
[50] Canadian Highway Bridge Design Code CAN/CSA S6-06, Canadian Standards Association, Rexdale, ON, Canada, 2006.
[51] ACI Committee 440. Guide for the Design and Construction of Structural Concrete Reinforced with FRP Bars Reported ACI 440.1R-06. Detroit: 2006.
[52] D. De Domenico, G. Ricciardi, Shear strength of RC beams with stirrups using an improved Eurocode 2 truss model with two variable-inclination compression struts, Eng. Struct. 198 (2019), https://doi.org/10.1016/j.engstruct.2019.109359.
[53] N. Tošić, S. Marinković, I. Ignjatović, A database on flexural and shear strength of reinforced recycledaggregate concrete beams and comparison to Eurocode 2 predictions, Constr. Build. Mater. 127 (2016) 932–944, https://doi.org/10.1016/j.conbuildmat.2016.10.058.
[54] Ali A.H., Mohamed H.M., Chalioris C.E., Deifalla A. Evaluating the shear design equations of FRP-reinforced concrete beams without shear reinforcement. Engineering Structures 2021;235. https://doi.org/10.1016/j.engstruct.2021.112017.
[55] T.G. Wakjira, A. Al-Hamrani, U. Ebead, W. Alnahhal, Shear capacity prediction of FRP-RC beams using single and ensenble explainable machine learning models, Compos. Struct. 287 (2022), https://doi.org/10.1016/j.compstruct.2022.115381.
[56] A. Younis, U. Ebead, P. Suraneni, A. Nanni, Performance of sewater-mixed recycled-aggregate concrete, J. Mater. Civ. Eng. 32 (2020), 04019331.
[57] M. Etxeberria, A. Gonzalez-Corominas, P. Pardo, Influence of seawater and blast furnace cement employment on recycled aggregate concretes' properties, Constr. Build. Mater. 115 (2016) 496–505, https://doi.org/10.1016/j.conbuildmat.2016.04.064.
[58] A. Younis, U. Ebead, P. Suraneni, A. Nanni, Fresh and hardened properties of seawater-mixed concrete, Constr. Build. Mater. 190 (2018) 276–286, https://doi.org/10.1016/j.conbuildmat.2018.09.126.
[59] BS EN 206, Concrete specification, performance, Production and Conformity, BSI, 2013.
[60] R.V. Silva, J. De Brito, R.K. Dhir, Fresh-state performance of recycled aggregate concrete: a review, Constr. Build. Mater. 178 (2018) 19–31, https://doi.org/10.1016/j.conbuildmat.2018.05.149.
[61] ATP Construction Composites. Data sheet for GFRP rebars 2019. http://www.atp-frp.com/html/products_tds.html#rwb-v.
[62] A. Cladera, A. Marí, J.M. Bairán, C. Ribas, E. Oller, N. Duarte, The compression chord capacity model for the shear design and assessment of reinforced and prestressed concrete beams, Structural Concrete 17 (2016) 1017–1032, https://doi.org/10.1002/suco.201500214.
[63] L. Butler, J.S. West, S.L. Tighe, The effect of recycled concrete aggregate properties on the bond strength between RCA concrete and steel reinforcement, Cem. Concr. Res. 41 (2011) 1037–1049, https://doi.org/10.1016/j.cemconres.2011.06.004.
[64] F. Yan, Z. Lin, M. Yang, Bond mechanism and bond strength of GFRP bars to concrete: a review, Composites Part B: Eng. 98 (2016) 56–69, https://doi.org/10.1016/j.compositesb.2016.04.068.
[65] M. Behera, S.K. Bhattacharyya, A.K. Minocha, R. Deoliya, S. Maiti, Recycled aggregate from C&D waste & its use in concrete - A breakthrough towards sustainability in construction sector: a review, Constr. Build. Mater. 68 (2014) 501–516, https://doi.org/10.1016/j.conbuildmat.2014.07.003.
[66] S. Seara-Paz, B. González-Fonteboa, J. Eiras-López, M.F. Herrador, Bond behavior between steel reinforcement and recycled concrete, Mater. Struct./Materiaux et Constructions 47 (2013) 323–334, https://doi.org/10.1617/s11527-013-0063-z.
[67] M. Krall, M.A. Polak, Concrete beams with different arrangements of GFRP flexural and shear reinforcement, Eng. Struct. 198 (2019), https://doi.org/10.1016/j.engstruct.2019.109333.
[68] A. Younis, U. Ebead, P. Suraneni, A. Nanni, Short-term flexural performance of seawater-mixed recycled-aggregate GFRP-reinforced concrete beams, Compos. Struct. 236 (2020), 111860, https://doi.org/10.1016/j.compstruct.2020.111860.
[69] ACI Committee 440, Guide For the Design and Construction of Structural Concrete Reinforced With FRP Bars (ACI 440.1 R-15), American Concrete Institute, 2015.
[70] Canadian Standards Association. CSA S806-12 design and construction of building structures with fibre-reinforced polymers. 2012.
[71] ISIS Canada Corporation. ISIS design manual: reinforcing concrete structures with fiber reinforced polymers-design manual No. 3. Manitoba, Canada: 2007.
[72] ASTM C143/C143M-15a: Standard test method for slump of hydraulic-cement concrete. ASTM International; 2015.
[73] ASTM C138/C138M-17: Standard test method for density (Unit Weight), yield, and air content (gravimetric) of concrete. ASTM International; 2017.
[74] C39/C39M-16b AIA, ASTM C39/C39M-16b: Standard test Method For Compressive Strength of Cylindrical Concrete Specimens, ASTM International, West Conshohocken, PA, PA, 2016.
[75] ASTM International. C78/C78M-18 Standard test method for flexural strength of concrete (using simple beam with third-point loading). West Conshohocken, PA: ASTM International; 2018. https://doi.org/10.1520/C0078_C0078M-18.